

# Nanophotonics for Information Systems

**Y. Fainman**

*Dept. of Electrical and Computer Engineering, UC–San Diego  
9500 Gilman Drive, La Jolla, California, 92093-0407, U.S.A.*

## 1. Introduction

Optics has the potential to solve some of the most pressing problems in communication and computing hardware. It promises crosstalk-free interconnects with essentially unlimited bandwidth; long-distance data transmission without skew and without power- and time-consuming regeneration; miniaturization; parallelism; and efficient implementation of important algorithms such as Fourier transforms. In the past, when the speed of digital computers was able to support only relatively small information processing throughput, optical information processing techniques were developed and used to construct processors and systems in support of numerous applications that required high throughput for real time operation. These methods exploited the parallelism of optics supported by the richness of the modal continuum of free space and a variety of optoelectronic devices that were developed in support of these applications and systems. The constructed information processing systems and concepts were used for image processing,<sup>1-4</sup> pattern recognition,<sup>5,6</sup> neural networks,<sup>7</sup> and linear algebra calculus<sup>8</sup> – to name a few. However with rapid advancements of the speed and, therefore, the information processing throughput of digital computers, the optical signal processing systems were not able to support these applications in a broad sense due to high cost, lesser accuracy, and lack of user-friendly interfaces. Later, the optical information processing transformed from parallelism in space domain to parallelism in optical frequency domain in support of processing information carried by ultrashort optical pulses in the femtosecond range. Such waveforms vary too rapidly for even the fastest photodetectors to resolve, leading to the need to develop optical information processing methods. Time-domain and spectral-domain processors utilized linear<sup>9</sup> and nonlinear<sup>10</sup> processes, and found useful applications for ultrafast waveform synthesis, detection and processing.<sup>10-12</sup>

It is evident that optical processing in space and time has so far failed to move out of the lab. The free-space and guided-wave devices are costly, bulky, and fragile in their alignment. They are also difficult to integrate with electronic systems, both in terms of the fabrication process and in terms of delivery and retrieval of the massive volumes of data the optical elements can process. However, with the most recent emphases on construction of *chip-scale integration* using advanced lithographic tools employed in surrounding electronics, things may be changing. Experts predict lithographic resolution as fine as 16 nm by the year

2020, which is about a hundred times smaller than the telecommunication wavelength of 1550 nm. These techniques can be used to create deeply subwavelength features that act as *metamaterials* with optical properties controlled by the *density* and *geometry* of the pattern and its *constituent materials*. In this Section we focus on metamaterials composed primarily of dielectrics that are engineered on the nanometer scale so as to have emergent optical properties not otherwise present. The increased localization of the optical field as a result of these engineered materials brings about phenomena such as form-birefringence, structural dispersion and enhanced optical nonlinear interactions. Equivalently, characteristics such as the local polarizability and dispersion of the metamaterial may be controlled by geometry, properties of constituent materials and their composition. The introduction of periodicity into these engineered materials modifies the dispersion relations and can be used to create an artificial bandgap.<sup>13-15</sup> The manipulation and modification of this periodicity allows the bandgap to shift and parts of the bandgap to be accessed by propagating modes. Photonic crystal (PhC) waveguides rely on this exact concept – a line of defects is introduced into the otherwise periodic structure so as to guide light.<sup>16-18</sup> The confinement of light within the PhC lattice is also used to realize devices such as super collimators, super prisms, super lenses, omnidirectional filters, modulators and lasers through proper design and optimization of Bloch modes.<sup>19-28</sup>

Similar to the PhC in its periodic nature is a class of metamaterials that exploit the advantages of both continuous free-space and discrete guided-wave modes. The simplest example involves the propagation of light in a waveguiding slab, where confinement occurs only in the vertical direction; the free space propagation occurs in the plane of the slab. This configuration, aptly termed "free space optics on a chip" (FSOC), enables interaction with discrete optical components that are located along the propagation direction. Functionalizing devices for such integrated systems would require free space implementations of focusing, beam steering, and wavelength selectivity.<sup>29</sup> Realization of these functionalities can exploit periodic, quasi-periodic or even random nanostructured composites. By altering the surface morphology of a dielectric on the nanoscale via nanolithography and advanced etching techniques, we can realize these complex structures and control the materials' local polarizability. As we shall see in this chapter, these structures fall into the deep sub-wavelength regime with spatial features  $\ll \lambda/2n$  and require metamaterial engineering with very high spatial resolution.

The engineering of composite dielectrics can continue to larger scales creating metamaterials that involve feature sizes on a larger sub-wavelength scale, e.g. just  $< \lambda/2n$ . The common themes of periodicity/quasi-periodicity and enhanced effects due to light confinement of guided modes will still remain. Continuing the simplification of PhC with periodicity in two dimensions that has been used for planar confinement, an alternative system whereby 2D light confinement is achieved by total internal reflection and 1D periodicity is introduced to create a bandgap in the third dimension. One method involves using a channel waveguide to guide light, rather than a slab waveguide as in the FSOC case, and periodically

modulating the effective index of the channel waveguide along the propagation direction. This results in a periodic quantum wire akin to a 1D PhC. Thereafter, interesting properties may be engineered by once again, introducing defects in the periodic structure to access forbidden modes or slightly changing the periodicity to alter the effective bandgap and dispersive properties. The strong confinement of fields in these engineered quantum wire-like structures will also enable interaction with other overlapping fields or discrete components despite the highly guided nature of these modes.

Silicon-on-insulator materials (SOI) and III-V compound semiconductor materials will be used for most of the discussion in this chapter because SOI is compatible with the well established CMOS fabrication process, and III-V semiconductors have been frequently used in heterogeneous integrated circuits and systems. In addition, the large index difference between silicon and its oxide leads to highly confined modes and enables the miniaturization of on-chip silicon-based photonic circuits. Furthermore, silicon is optically transparent and has a very low material absorption coefficient around the telecom wavelength  $\lambda = 1550$  nm. Waveguiding loss in SOI platforms has a state of the art value of less than 1 dB/cm. In terms of the impact for future systems applications, it is evident that next generation computing would benefit greatly from all-optical data transfer and processing on a chip. Electrical interconnections inherent in today's computing cannot measure up in terms of both speed and bandwidth. Researchers in the field are aware of the need to bypass any sort of electro-optic process in order to take computing speeds to the next level. Much work is being done in creating both passive and active devices in SOI. Discrete device components such as filters, modulators, and resonators have been demonstrated. Active devices utilizing Raman gain and hybrid silicon lasers, which achieve gain from a bonded III-V material, have also been demonstrated. The momentum of research in this area is the best evidence that silicon photonics is set to revolutionize the field of computing and communications.

In this chapter, we will divide the analysis of the dielectric metamaterials into two categories, namely those in the deep sub-wavelength and those in the larger, sub-wavelength scale. As we shall see, interesting emergent properties arise when the materials are engineered to sizes smaller than or comparable to the wavelength of light in the said medium. Optical field concentrators, compact sources, polarizers, chromatic dispersers, diffractive structures, and other optical processing devices can now be implemented on-chip using metamaterials wherever natural materials with similar properties either do not exist, or (more frequently) would not be compatible with lithographic fabrication processing. Moreover, there exists an opportunity to develop a new family of optical devices exploiting near-field interactions to a much greater extent than has been possible to date. In summary, there exist an opportunity in using advanced lithography and material composition to "lithographically right and assemble" optical materials and devices with *novel optical functionalities* into circuits and subsystems on a chip.

## 2. Nanophotonics process

To advance this technology, investigations of nanostructures and their interaction with electromagnetic field are critical. Engineers also need appropriate modeling and design tools, new fabrication recipes, and test instruments capable of characterizing on-chip components. The nanophotonics process will help to establish near-field optical systems science and underlying technologies to advance future integrated information systems.

The design of integrated photonic systems is a challenging task, as it not only involves the accurate solution of electromagnetic equations, but also the need to incorporate the material and quantum physics equations into the analysis of near-field interactions. These studies need to be integrated with device fabrication and characterization to verify device concepts and optimize device designs. In this chapter we discuss examples of SOI metamaterials and devices that can be realized using CMOS-compatible fabrication process that we demonstrated recently in our lab. These examples include birefringent elements that utilize a combination of geometry and material properties to separate light into orthogonal polarizations, graded-index lenses, frequency-selective resonators and Bragg gratings, and metal-dielectric nanostructures that can achieve extremely tight field confinement. Some of these example devices are tested using a near field characterization tool, the heterodyne near-field scanning optical microscope (H-NSOM). This microscope uses a fiber probe tapered to about 200–500 nm diameter with an aperture of about 50–200 nm, brought close enough to the nanostructure under test to pick up its evanescent electromagnetic fields. The idea to improve resolution of optical measurements by bringing a subwavelength aperture close to the object of interest was first introduced by Syngge in 1928 and experimentally realized only in 1983 by two independently working research groups: Dieter W. Pohl and co-workers at IBM<sup>30</sup> and Aaron Lewis and co-workers at Cornell University.<sup>31</sup> The efficiency of light transmission  $T$  through a small aperture ( $d \ll \lambda$ ) drops rapidly<sup>31</sup> as the aperture size decreases,  $T \sim (d/\lambda)^4$ . Thus, for realistic aperture of 100 nm and visible wavelengths the transmission efficiency only reaches  $10^{-6}$ – $10^{-8}$ .<sup>32</sup> Such small transmission coefficients demand the use powerful optical sources (often lasers), efficient detection schemes, and detectors. One example of a suitable detection scheme is heterodyne detection, an interferometric technique that not only improves the detection efficiency but also allows measurement of optical phase.

The concept of heterodyne detection is to mix the signal of interest with a coherent reference beam at a slightly shifted optical frequency. This can be done via a Mach-Zehnder interferometer with one (signal) arm including NSOM and the other (reference) arm providing a frequency-shifted reference. The two fields are added coherently, yielding the desired interference signal oscillating at the heterodyne frequency. The coherent gain of the heterodyne detection significantly improves the sensitivity of the instrument.<sup>33</sup> The system is built from readily available telecom components. This in-fiber realization provides better interferometric stability; polarization-maintaining fibers can also be used for maximizing interference term.

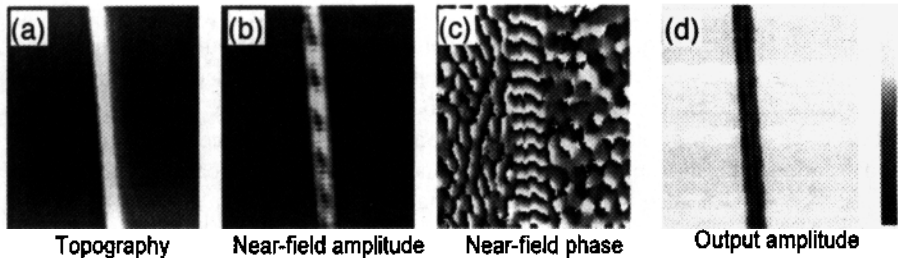


**Figure 1.** (a) Waveguide topography obtained in NSOM measurements; (b) and (c) near-field amplitude and phase distributions (respectively); and (d) output amplitude vs. position of the NSOM tip.

The scanning process provides simultaneously three images: sample topography, deduced from the AFM feedback system that keeps the probe at a constant height above the sample surface; and amplitude and phase distributions of the evanescent optical fields. Example of H-NSOM characterization of an SOI waveguide is shown in Fig. 1. The mapping of evanescent fields has proven to be a powerful tool in understanding the performance of nanoscale optical materials, devices, and circuits.

### 3. Dielectric metamaterials

In this Section, we will describe the analysis of deep sub-wavelength scale dielectric metamaterials and their behavior in the sub-wavelength scale limit, as well as when they are perturbed into aperiodic composites.

We investigate a class of dielectrics, characterized by feature sizes  $\delta \ll \lambda/2n$ , where  $\lambda$  is the free-space wavelength and  $n$  is the refractive index of the dielectric material. Photonic structures with periodic or quasi-periodic refractive index variations on a scale much smaller than the wavelength of light can be called "metamaterials" (from the Greek word "μετά", meaning "after" or "beyond") – materials whose optical properties arise from structural geometry rather than only from the composition of constituent materials. This approach, as we will discover in detail in this Section, can be illustrated by the simplest example of form-birefringent materials: 1D periodic structures that have a polarization-dependent index of refraction<sup>34–36</sup> and unusual nonlinear properties.<sup>37,38</sup>

Form birefringence occurs in structures that have deep subwavelength periodicity.<sup>18</sup> The altered surface morphology of the dielectric used to construct such structures results in a large difference between the effective indices of the TE and TM polarized optical fields, since they need to satisfy different boundary conditions. Form-birefringent nanostructures (FBNs) go beyond naturally birefringent materials in (i) the strength of birefringence  $\Delta n/n$  (where  $\Delta n$  is the difference in the refractive index for the two orthogonal polarizations); (ii) the extent of form birefringence  $\Delta n$  that may be adjusted by varying the duty cycle as well as the shape of the microstructures; and (iii) the possibility of modifying the

reflection properties of dielectric boundaries.<sup>39</sup> These features are useful for constructing polarization-selective beam splitters and general-purpose polarization-selective diffractive optical elements such as birefringent computer-generated holograms.<sup>36</sup> Extending this concept to the 2D geometry or implementing aperiodicity enables other useful functionalities, such as converting a linear polarization state to radial or azimuthal polarization<sup>39,40</sup> and creating graded-index media.<sup>40,41</sup> It was also shown that metamaterial approach can help to overcome fabrication difficulties and create a Fresnel lens analogue using binary lithographic fabrication with deep subwavelength feature sizes of less than 60 nm.<sup>29</sup>

It is also possible to mold the light flow in the planar configuration by using metamaterials. Bringing the functionality of tabletop optical information processing components to a chip will create compact devices, which can benefit from fast data transfer, small form-factor, parallel processing, and low power consumption. Implementing free-space-like propagation for planar optics means that while the light is confined by index difference in the vertical direction (chip plane), the horizontal beam size is regulated by phenomena similar to the diffraction, reflection and refraction of 3D free-space optics. This can be seen as a direct and more natural transition of the conventional free-space bulk optical components and devices to the chip-scale of photonic integrated circuits.

To create a dielectric metamaterial we use a subwavelength structure that can be fabricated in the high refractive index slab – see Fig. 2(a). The slab has an index of refraction  $n_1$ , while the gaps in the etched subwavelength structure can be filled with a material possessing a lower index of refraction  $n_2$ , e.g. air with  $n_2 = 1$ . This slab structure is constructed on the cladding with an overall lower index of refraction  $n_c < n_1$ , to ensure confinement in the vertical direction. For some material systems, such as SOI, the cladding with the guiding slab is located on top of a thick substrate with the refractive index  $n_s$ . Consider a grating with a period  $\Lambda$ , where  $F\Lambda$  is the fraction of the unit cell filled with high-index material. It can be shown that the second-order effective medium theory approximation<sup>42,43</sup> is accurate for small grating periods  $\Lambda < \lambda/n$ <sup>18</sup> and for grating thickness larger than  $\lambda/3$ .<sup>44</sup> Other approaches in design and analysis of these subwavelength grating metamaterial structures include numerical methods such as RCWA, finite element method (FEM), and the finite-difference time-domain (FDTD) approaches.

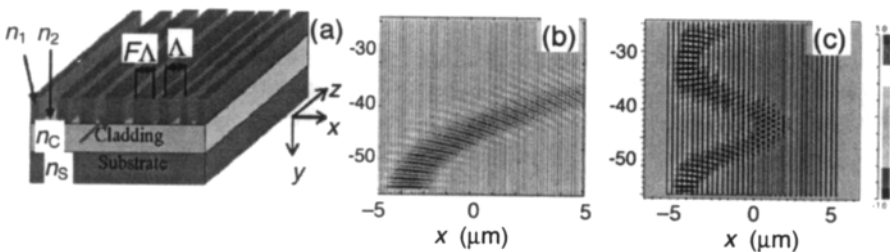


**Figure 2.** Schematic diagram of a subwavelength planar metamaterial: (a) description of a deeply subwavelength approach to dielectric metamaterial structure; Numeric simulation results showing light propagation in subwavelength SOI gratings with spatial chirp introduced by linearly varying the filling factor (increasing from left to right) and initial periods of (b)  $\Lambda = 150$  nm and (c)  $\Lambda = 300$  nm.

This concept can be used to create new materials with refractive indices different from those of the constituent materials. For example, for the SOI material system, we usually have silicon with index of refraction of  $n_{\text{Si}} = 3.48$  and silicon dioxide with  $n_{\text{SiO}_2} = 1.46$  as the only materials available for structure design. On the other hand, in the tabletop free-space optics space we have access to a variety of other materials: different glasses, crystals, polymers, *etc.* This fact makes it difficult to directly translate tabletop optical setups to on-chip implementations. Metamaterials can provide a solution to overcome this difficulty. For example, by fabricating a subwavelength grating, the achievable index in SOI varies from 1.5 to 3.4, thus covering almost fully the range between high-index silicon and low-index oxide. This range was estimated for TE-polarized fields in structures with a period of  $\Lambda = 400$  nm satisfying the  $\Lambda < \lambda/n = 1500 \text{ nm}/3.5 \sim 400$  nm condition, with filling factors varying from 0.1 to 0.9 to comply with the state-of-the-art nanofabrication capabilities (feature size  $\sim 40$  nm).

Next we examine a subwavelength structure with a linearly varying filling factor. Such a slab will equivalently act as a graded-index metamaterial, where the effective index of refraction in the transverse direction decreases or increases linearly. It is well known that in such a "graded" index material, the incident beam of light will bend towards the higher index of refraction. We performed numerical simulations of light propagation in such a spatially chirped subwavelength grating structure with the initial periods  $\Lambda = 150$  and 300 nm. The numeric simulation results for SOI material platform are summarized in Fig. 2(b) and (c). The propagation of light for the structure the shorter initial period (deep sub-wavelength limit at  $\Lambda = 150$  nm) shows truly graded index behavior – see Fig. 2(b). Conversely, for the larger initial period  $\Lambda = 300$  nm we can observe some reflection – see Fig. 2(c) – with a "snake-like" propagation trajectory due to Bragg reflection. That is, as the light beam propagates close to the normal to the refractive index gradient, its effective wavelength becomes smaller (as the index increases) until the Bragg matching condition is satisfied when  $\lambda_{\text{eff}} = \Lambda/n = 2\Lambda \sin\theta$  (for the first diffraction order). After the Bragg-matched reflection, the light beam propagates towards the lower effective refractive index in the graded medium. Consequently, the "total internal reflection" condition will be satisfied and the light beam will be reflected back again. This type of "snake-like" light propagation occurring due to a combination of nonresonant and resonant transient metamaterial behavior is quite unusual and cannot be observed in natural materials.

An example of using such a nonresonant metamaterial that can dramatically affect the dispersive properties of the propagating light<sup>45</sup> for a specific application is the mode-matching device, where position-dependent polarizability to guide and manipulate the modes of light propagating on a chip. The device is realized by lithographically defining and etching subwavelength features into a high-refractive-index slab waveguide,<sup>29</sup> modifying its local effective index of refraction. We use a subwavelength periodic structure and locally modulate its duty cycle in the transverse direction  $x$ , to achieve modulation of the index of refraction, i.e.  $n(x) = n_0(1 - \alpha x^2/2)$ , where  $n_0$  and  $\alpha$  are constants representing the maximal effective index and the gradient strength, respectively. To validate our approach, we

designed and fabricated a graded index slab element that focuses light into a 2  $\mu\text{m}$  wide Si ridge waveguide. We used an SOI wafer with a Si slab thickness of 250 nm and an oxide thickness of 3  $\mu\text{m}$ . The fabricated element in Fig. 3 shows the layout of the device. A grating period of 400 nm was chosen to assure the validity of the effective medium approximation on one hand, and to avoid the need for fabricating ultra small features. For compatibility with CMOS fabrication, the minimal air gap was chosen to be 100 nm, imposing a maximal duty cycle of 75%. An SEM micrograph showing the layout of the entire fabricated device is depicted in Fig. 3.

Typically, characterization of nanophotonic devices is performed by analyzing the light intensity at the output of the device. Unfortunately, this approach lacks the ability to probe the amplitude and, even more importantly, the phase profile of the optical beam as it propagates within the structure. To overcome this problem, the fabricated samples were characterized with the H-NSOM,<sup>33</sup> capable of measuring both amplitude and phase of the propagating optical field with a resolution of about 100 nm. Figure 4 shows the measured amplitude and phase of the optical field propagating through the device at a wavelength of  $\lambda = 1550$  nm. Figure 4(a) shows the amplitude of the optical field in the region that includes the input waveguide, the non-patterned slab ("S") and large portion of the slab lens section ("L"). The dashed vertical white lines mark the boundaries between the various sections of the device. Light propagates from left to right. Figure 4(b) shows the measured phase in the same region. Figure 4(c) shows several cross-sections of the phase front calculated from Fig. 4(b) at several planes along the  $z$ -axis. The obtained results clearly show the expansion of the optical beam in the region of the slab. As expected, the phase front is diverging in this section. As the beam enters the metamaterial, the curvature of the phase front gradually decreases and becomes planar after about 5  $\mu\text{m}$  propagation in the slab. Then, the phase front begins to converge towards the focus. As the beam continues to propagate, the phase front starts to diverge again, and the optical beam expands.

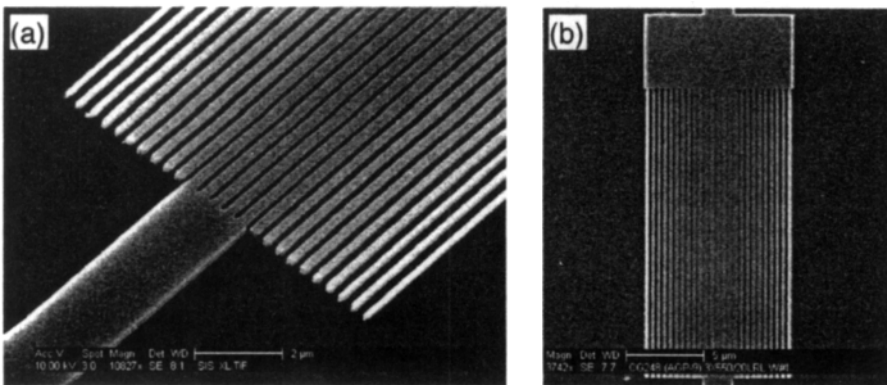


**Figure 3.** Scanning electron micrograph showing the fabricated device: (a) top view of the entire structure; (b) magnified slanted view showing part of slab lens and the output waveguide.<sup>29</sup>

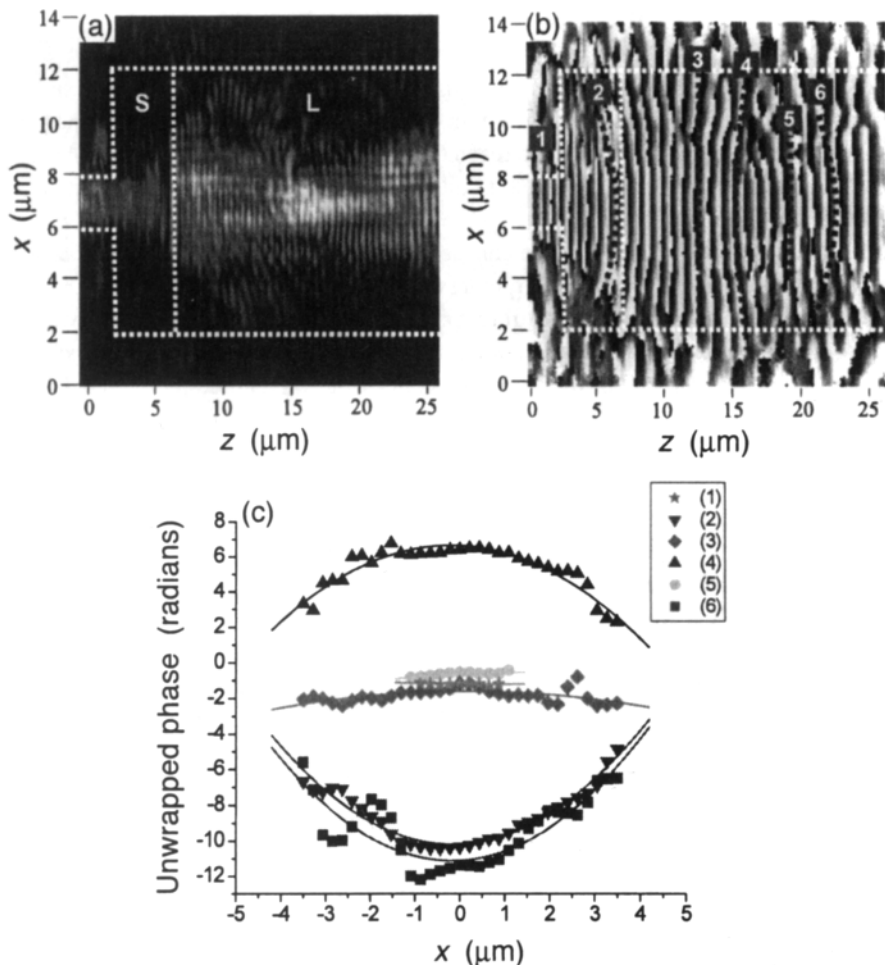


**Figure 4.** Experimental results obtained with the H-NSOM: (a) amplitude and (b) phase of the optical field in the region that includes the input waveguide, the non-patterned slab ("S") and large portion of the slab lens section ("L"). The dashed vertical white lines mark the boundaries between the various sections and light is propagating from left to right. (c) Cross sections showing phase profile at several planes along the device marked in (b).<sup>29</sup>

The investigated metamaterial-based graded-index slab "lens" device is the first step towards the realization of the FSOC concept. Our H-NSOM measurements clearly demonstrate the focusing effect. This experimental demonstration opens new possibilities in the field of on-chip photonic integration, as the demonstrated component can be integrated with other building blocks (some yet to be developed) to create future devices and systems based on the FSOC concept. We believe that this new concept may become essential for applications such as optical interconnections, information processing, spectroscopy and sensing on a chip.

#### 4. Quantum wires: Subwavelength inhomogeneous dielectrics

We refer to sub-wavelength structures as structures with features that are smaller than but comparable to the wavelength of light. An example of such periodic structures is a general family of resonant structured materials such as photonic crystal (PhC) lattices and the whole family of devices that can be implemented in a PhC lattice. In this section we explore a novel practical approach that we call quantum wire metamaterials that can be used to implement both subwavelength and deep subwavelength nanostructures. We recall that subwavelength scale devices are characterized by feature sizes  $\Lambda < \lambda/2n_{\text{eff}}$ , where  $\lambda$  is the vacuum wavelength and  $n_{\text{eff}}$  is the effective index of the specific mode in the device:  $n_{\text{eff}} = \beta/k$ , where  $\beta$  is the propagation constant of the waveguide mode and  $k$  is the wave number in vacuum. For example, for the SOI material system, we can construct a typical single-mode silicon waveguide with  $n_{\text{eff}} \sim 2.5$  for operation at the telecommunications wavelength of 1.55  $\mu\text{m}$ . In the following, we will mainly focus on the subwavelength regime to demonstrate the unique capabilities of this approach and demonstrate experimental device prototypes. We first investigate a periodic 1D PhC quantum wire, and extend the investigation to a quasi-periodic quantum wire. Finally, we study the characteristics of a filter created by coupling two such quantum wires together.

The PhC lattice<sup>13-15</sup> is a well known resonant inhomogeneous material, which has been fabricated in many ways during the past decade.<sup>19,20,35,46</sup> It may play a unique role as an integration platform of nanophotonic devices, as numerous PhC-based devices with various functionalities have been reported, including modulators, detectors, filters, lasers, superprisms and elements with negative refraction. However, fabrication of 3D resonant inhomogeneous materials and devices remains challenging, and frequently, 1D and 2D topologies are used due ease in their design, fabrication and integration. A simple example of a 1D resonant structure is a distributed Bragg reflector (DBR) used in planar waveguide technology to perform and enhance various functionalities of optical elements, such as a single-mode selector in semiconductor lasers, optical filters, switches, modulators, couplers, detectors, and sensors. The DBRs conventionally fabricated on the surface of the waveguide involve an additional fabrication procedure separate from the waveguide. Recently, in contrast to traditional approaches, we exploited a single-step fabrication method to define the DBRs and other nanostructured resonant devices using the corrugation of waveguide sidewalls. In this approach, both the period and the modulation strength of the DBRs are lithographically assigned on the waveguide sidewalls.<sup>47-49</sup>

The designed devices are Fabry-Perot (FP) type filters made of a pair of identical Bragg reflectors each having reflection ( $r$ ) and transmission ( $t$ ) amplitude coefficients, and separated by a spacer of length  $d = \Lambda/2$  causing a phase shift  $\phi = \pi/2$ . The transmission amplitude of the resonant filter  $t_{\text{RF}}$  as a function of  $\lambda$  is given by  $t_{\text{RF}} = t^2 \exp[i\phi] / (1 - r^2 \exp[i2\phi])$ . These filters are fabricated on a piece ( $\sim 1 \times 0.5 \text{ cm}^2$ ) of 6" SOI wafer consisting of a silicon top layer with a mean thickness of 252.2 nm with distribution of  $6\sigma \sim 18.3 \text{ nm}$  on a  $\sim 3 \mu\text{m}$  thick silicon dioxide layer.

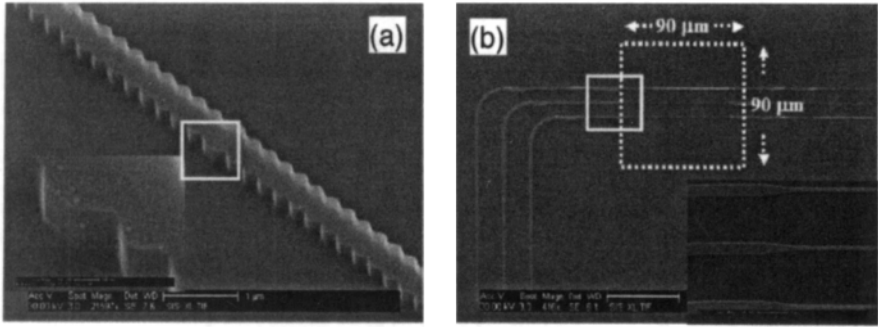


**Figure 5.** SEM micrographs of the devices. Insets of each figure show the magnified view of the rectangles: (a) transmission resonant filter with vertical gratings; (b) micrograph of the whole device and its inset showing the waveguide connection defined at two different magnifications. Dotted rectangle shows the area defined at  $\times 1000$  magnification.<sup>47,48</sup>

A tilted SEM image of the fabricated vertical grating filter is shown in Fig. 5(a). Figure 5(b) shows the micrograph of the entire device, whereas the inset of the Fig. 5 shows the magnified view of the tapered waveguide connections. The device is tested by coupling a linearly polarized tunable laser source into a polarization maintaining (PM) tapered fiber with an output spot diameter of  $\sim 2.5 \mu\text{m}$ , producing  $\sim 20$  dB polarization extinction. Another PM tapered fiber was used to collect light from the fabricated devices and its relative power transmission over the wavelength is analyzed. All measurements were performed using TE polarization. Figure 6 shows the measured transmission spectra of a fabricated device with a wide stopband of  $\sim 19$  nm bandwidth containing a narrow transmission band of linewidth  $\Delta\lambda \sim 0.5$  nm in the center of the stopband. The developed fabrication procedures show very good surface quality, which is also indicated by the measured value of cavity  $Q \sim \lambda_B/\Delta\lambda$  of about 3000.

The described resonant PhC-based devices and components implemented using quantum wires are essential for future integration of various information systems on a chip. The introduced graded index device is the first step towards the realization of devices based on near-field optical interactions using space variant polarizability. Moreover, a resonant nanophotonic device utilizing vertical gratings has been realized on an SOI wafer via a fabrication procedure that maintains good surface quality. These experimental demonstrations open new possibilities in the field of on-chip integrated photonic devices, as the demonstrated component can be combined with other building blocks to create future devices and systems based on the concept of free-space optics on a chip. Finally, the use of lithography for sidewall modulation is opening numerous opportunities in constructing various resonant devices for detection, modulation, generation, and manipulation of light on a chip.

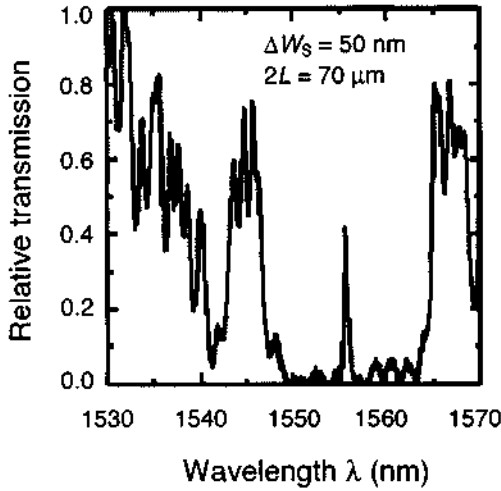


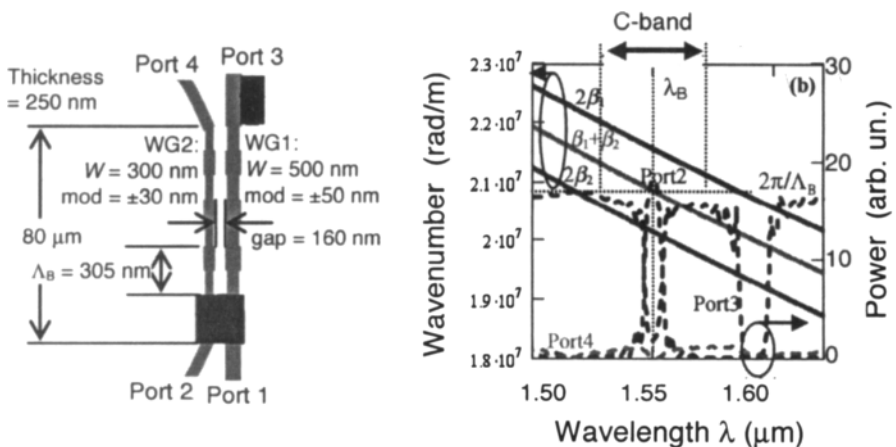
**Figure 6.** Measured spectra from the fabricated devices with  $W_S = 500 \text{ nm}$  and  $\Lambda = 305 \text{ nm}$  for  $\Delta W_S = 50 \text{ nm}$ ,  $2L = 70 \mu\text{m}$ .<sup>47, 48</sup>

### 5. Nanophotonic devices and circuits: Wavelength selective add drop filter with vertical gratings on silicon chip

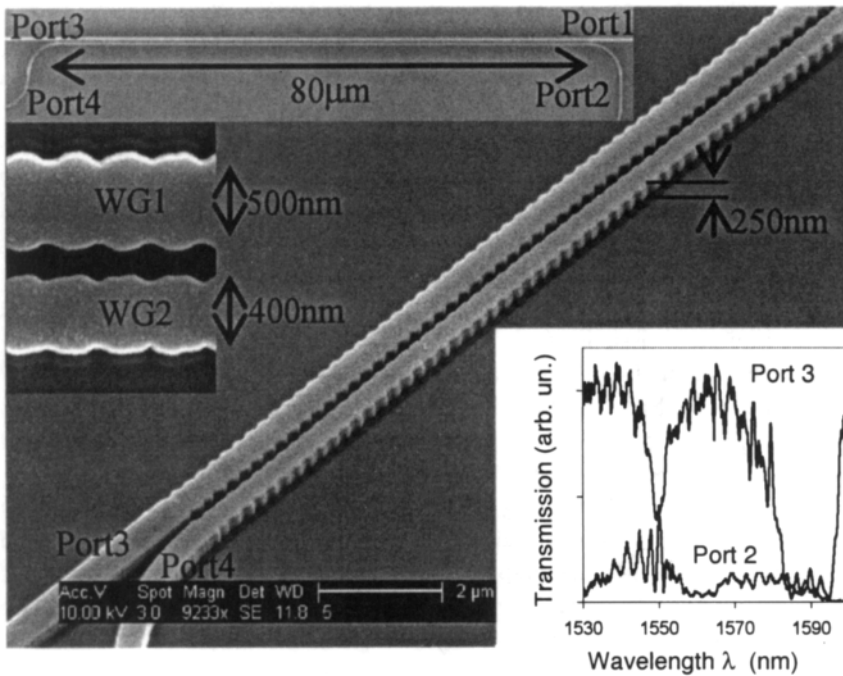
The SOI material platform is of great interest for information systems integration because it is compatible with the well-established CMOS fabrication process. Additionally, III-V semiconductors have been frequently used in heterogeneous integrated circuits and systems. Furthermore, silicon is optically transparent and has a very low material absorption around the telecommunications wavelength of  $1.55 \mu\text{m}$ . Waveguiding loss in SOI platforms has a state-of-the-art value of less than  $1 \text{ dB/cm}$ . In terms of the impact for future systems applications, it is evident that next generation computing would benefit greatly from all-optical data transfer and processing on a chip. Electrical interconnections inherent in today's computing cannot measure up in terms of both speed and bandwidth. Researchers in the field are aware of the need to bypass all electro-optic processes in order to take computing speeds to the next level.<sup>50</sup> Much work is being done in creating both passive and active devices in SOI. Discrete device components, such as filters, modulators, and resonators have been demonstrated. For example, the device described in Fig. 5 can serve a near-universal platform, but it somewhat suffers from the limited spectral bandwidth of the stopband of the sidewall-modulated quantum wire which is limited by the achievable effective index modulation. To achieve a larger stopband we need to increase the modulation, but this would cause increased scattering losses that will reduce the quality of the resonator. In this Section, we describe an alternative approach based on a wavelength-selective coupler (WSC) with vertical gratings on silicon chip.<sup>51</sup>

Figure 7(a) shows a schematic diagram of the WSC. We design the structure with three Bragg conditions:<sup>52</sup>  $2\beta_1(\lambda) = 2\pi/\Lambda$ , producing backward coupling in waveguide 1 (WG1);  $2\beta_2(\lambda) = 2\pi/\Lambda$ , producing backward coupling in WG2; and  $\beta_1(\lambda) + \beta_2(\lambda) = 2\pi/\Lambda$  (cross coupling), where  $\beta_1$  and  $\beta_2$  are the propagation constants of WG1 and WG2 respectively, and  $\Lambda$  is the period of the grating. Here, we allocate the cross-coupling wavelength to  $\lambda_B = 1.55 \mu\text{m}$  as a desired channel wavelength by setting the period as  $\Lambda_B = 2\pi/[\beta_1(\lambda_B) + \beta_2(\lambda_B)]$ , and backward coupling wavelengths in WG1 and WG2 to outside of C-band by setting  $2\beta_1(\lambda > 1.57 \mu\text{m}) = 2\pi/\Lambda_B$  and  $2\beta_2(\lambda < 1.53 \mu\text{m}) = 2\pi/\Lambda_B$ . Figure 7(b) shows the plots of  $2\beta_1$ ,  $2\beta_2$  and  $(\beta_1 + \beta_2)$  vs. wavelength (calculated with the effective index method), together with transmission spectrum from two-dimensional FDTD method (input at Port 1). The structure dimensions are described in Fig. 7(a) and all the calculations here are performed for the quasi-TE mode. We can see that in this design, we obtain the cross coupling with around 9 dB extinction at  $1.55 \mu\text{m}$  and the backward couplings outside the C-band at  $1.52 \mu\text{m}$  and  $1.59 \mu\text{m}$ .

We fabricated the WSC designed above using e-beam writing and reactive ion etching processes on an SOI wafer with  $3 \mu\text{m}$  buried oxide layer and  $250 \text{ nm}$  silicon layer. The SEM micrographs of the fabricated structure are shown in Fig. 8. After depositing the over-cladding  $\text{SiO}_2$  layer of  $2 \mu\text{m}$  thickness, we measured the transmission spectrum using a broadband light source input at Port 1 and a spectrum analyzer (see the inset of Fig. 8). We observe that the measured spectrum at Port 2 and 3 are in good agreement with the simulated spectrum. In order to further improve the extinction, we simply increase the total length or the waveguide modulation, or decrease the gap between the waveguides. And also, we could extend this device to multi-port add-drop device with placing another waveguide on the other side of the WG1 and/or cascading the WSCs.



**Figure 7.** (a) Schematic diagram and detail dimensions of WSC with vertical gratings; (b) plots of three Bragg conditions and transmission spectrum from 2D FDTD.<sup>51</sup>



**Figure 8.** SEM micrographs of the fabricated WSC and measured transmission spectrum at Port 2 and 3.<sup>51</sup>

## 6. Discussion and future perspectives

This chapter has given an introductory view on the emerging field of nanophotonics and its potential for chip-scale integration of information systems. The main points include our ability to use standard and emerging nanofabrication tools to create complex geometries of composite materials varying the spatial distributions periodically, quasi-periodically or even at random. The feature sizes of these nanocomposites can be deeply subwavelength, which enables creation of materials and devices with unique functionalities that are impossible to achieve with existing technologies. Moreover, the subwavelength structures can incorporate coupled devices operated in spatial as well as spectral resonance. We have described the localized effects and alterations in optical behavior of dielectric metamaterials with space-variant polarizability (form birefringence, snake-like propagation, and metamaterial lensing), as well as various functionalities achieved in single and spatially-coupled resonant quantum wires.

The current trend of using the SOI material platform will continue due to its compatibility with well-established CMOS fabrication, which is projected to reach resolution on the order of 10–16 nm in the near future. Another major reason is

that future computing systems complexity will increasingly rely on optical interconnections, possibly including intra-chip communications, where silicon photonics will enable efficient manipulation, transformation, filtering and detection of light meeting the needs of the future information systems. It should be noted that efficient generation of light on a silicon chip is still in its infancy and may not be able to overcome the fundamental problem of the indirect bandgap, but alternative solutions similar to delivery of electrical power from off-chip sources will bring optical fields into Si chips. Progress in heterogeneous metamaterials is certainly another valid alternative, but it may require major technological and manufacturing breakthroughs. It is evident that the fundamental limits of scale and composition in the present technology will continue to shift to ever smaller features and ever more complex material compositions. It is possible that current trends in engineering electronic bandgaps are not merely a pipe dream, and may one day merge with engineered nanophotonic metamaterials, leading to new device concepts that will serve as the backbone of future information systems technologies. Engineering the polarizability of dielectric nanostructures is still in its nascent stages and numerous novel functionalities are still to come.

## References

1. Y. Fainman, E. Klancnik and S. H. Lee, "Optimal coherent image amplification by two beam coupling in photorefractive BaTiO<sub>3</sub>," *Opt. Eng.* **25**, 228 (1986).
2. Y. Fainman, C. C. Guest, and S. H. Lee, "Optical digital logic operations by two beam coupling in photorefractive material," *Appl. Opt.* **25**, 1598 (1986).
3. P. Ambs, S. H. Lee, Q. Tian, and Y. Fainman, "Optical implementation of the Hough transform by a matrix of holograms," *Appl. Opt.* **25**, 4039 (1986).
4. P. Ambs, Y. Fainman, S. H. Lee, and J. Gresser, "Computerized design and generation of space-variant holographic filters. Part I: System design considerations and applications of space-variant filters to image processing," *Appl. Opt.* **27**, 4753 (1988).
5. Q. Tian, Y. Fainman, Z. H. Gu, and S. H. Lee, "Comparison of statistical pattern recognition algorithms for hybrid processing. Part I: Linear mapping algorithms," *J. Opt. Soc. Amer. A* **5**, 1655 (1988).
6. Q. Tian, Y. Fainman, and S. H. Lee: "Comparison of statistical pattern recognition algorithms for hybrid processing. Part II: Eigenvector-based algorithms," *J. Opt. Soc. Amer. A* **5**, 1670 (1988).
7. J. Y. Jau, Y. Fainman, and S. H. Lee: "Comparison of artificial neural network with pattern recognition and signal processing," *Appl. Opt.* **28**, 302 (1989).
8. H. Rajbenbach, Y. Fainman and S. H. Lee: "Optical implementation of an iterative algorithm for matrix inversion," *Appl. Opt.* **26**, 1024 (1987).
9. P. C. Sun, Y. Mazurenko, W. Chang, P. Yu, and Y. Fainman " All-optical parallel-to-serial conversion by holographic spatial-to-temporal frequency encoding," *Opt. Lett.* **20**, 1728 (1995).

10. P. C. Sun, Y. Mazurenko, and Y. Fainman, "Femtosecond pulse imaging: Ultrafast optical oscilloscope," *J. Opt. Soc. Amer. A* **14**, 1159 (1997).
11. D. M. Marom, D. Panasenko, P. C. Sun, and Y. Fainman, "Spatial-temporal wave mixing for space-time conversion," *Opt. Lett.* **24**, 563 (1999).
12. R. E. Saperstein, D. Panasenko, and Y. Fainman, "Demonstration of a microwave spectrum analyzer based on time-domain optical processing in fiber," *Opt. Lett.* **29**, 501 (2004).
13. J. D. Joannopoulos, S. G. Johnson, J. N. Winn, and R. D. Meade, *Photonic Crystals: Molding the Flow of Light*, 2nd ed., Princeton, NJ: Princeton University Press, 2008.
14. E. Yablonovitch, "Inhibited spontaneous emission in solid-state physics and electronics," *Phys. Rev. Lett.* **58**, 2059 (1987).
15. S. John, "Strong localization of photons in certain disordered dielectric superlattices," *Phys. Rev. Lett.* **58**, 2486 (1987).
16. M. Abashin, P. Tortora, I. Marki, *et al.*, "Near-field characterization of propagating optical modes in photonic crystal waveguides," *Opt. Express* **14**, 1643 (2006).
17. R. D. Meade, A. Devenyi, J. D. Joannopoulos, O. L. Alerhand, D. A. Smith, and K. Kash, "Novel applications of photonic band gap materials: Low-loss bends and high Q cavities," *J. Appl. Phys.* **75**, 4753 (1994).
18. I. Richter, P. C. Sun, F. Xu, and Y. Fainman, "Design considerations of form birefringent microstructures," *Appl. Opt.* **34**, 2421 (1995).
19. R. Tyan, P. C. Sun, A. Scherer, and Y. Fainman, "Polarizing beam splitter based on the anisotropic spectral reflectivity characteristic of form-birefringent multilayer grating," *Opt. Lett.* **21**, 761 (1996).
20. W. Nakagawa, P. C. Sun, C. H. Chen, and Y. Fainman, "Wide field of view narrow band spectral filter base on photonic crystal nanocavities," *Opt. Lett.* **27**, 191 (2002).
21. S. Lin, E. Chow, V. Hietala, P. R. Villeneuve, and J. D. Joannopoulos, "Experimental demonstration of guiding and bending of electromagnetic waves in a photonic crystal," *Science* **282**, 274 (1998).
22. H. Kosaka, T. Kawashima, A. Tomita, M. Notomi, T. Tamamura, T. Sato, and S. Kawakami, "Self-collimating phenomena in photonic crystals," *Appl. Phys. Lett.* **74**, 1212 (1999).
23. E. Schonbrun, Q. Wu, W. Park, T. Yamashita, C. J. Summers, M. Abashin, and Y. Fainman, "Wave front evolution of negatively refracted waves in a photonic crystal," *Appl. Phys. Lett.* **90**, 041113 (2007)
24. H. Kosaka, T. Kawashima, A. Tomita, M. Notomi, T. Tamamura, T. Sato, and S. Kawakami, "Superprism phenomena in photonic crystals: Towards microscale lightwave circuits," *Phys. Rev. B* **58**, R10096 (1998).
25. E. Schonbrun, M. Abashin, J. Blair, Q. Wu, W. Park, Y. Fainman, and C. J. Summers, "Total internal reflection photonic crystal prism," *Opt. Express* **15**, 8065 (2007).
26. C. Luo, S. G. Johnson, and J. D. Joannopoulos, "Subwavelength imaging in photonic crystals," *Phys. Rev. B* **68**, 045115 (2003).

27. Y. Fink, J. N. Winn, S. Fan, C. Chen, J. Michel, J. D. Joannopoulos, and E. L. Thomas, "A dielectric omnidirectional reflector," *Science* **282**, 1679 (1998).
28. O. Painter, R. K. Lee, A. Scherer, A. Yariv, J. D. O'Brien, P. D. Dapkus, and I. Kim, "Two-dimensional photonic band-gap defect mode laser," *Science* **284**, 1819 (1999).
29. U. Levy, M. Abashin, K. Ikeda, A. Krishnamoorthy, J. Cunningham, and Y. Fainman, "Inhomogeneous dielectric metamaterials with space-variant polarizability," *Phys. Rev. Lett.* **98**, 243901 (2007).
30. D. W. Pohl, W. Denk, and M. Lanz, "Optical stethoscopy: image recording with resolution  $\lambda/20$ ," *Appl. Phys. Lett.* **44**, 651 (1984).
31. A. Lewis, M. Isaacson, A. Harootunian, *et al.*, "Development of a 500 Å spatial resolution light microscope. I. Light is efficiently transmitted through  $\lambda/16$  diameter apertures," *Ultramicroscopy* **13**, 227 (1984).
32. G. A. Valaskovic, M. Holton, and G. H. Morrison, "Parameter control, characterization, and optimization in the fabrication of optical fiber near-field probes," *Appl. Opt.* **34**, 1215 (1995).
33. A. Nesci and Y. Fainman, "Complex amplitude of an ultrashort pulse with femtosecond resolution in a waveguide using a coherent NSOM at 1550 nm," *Proc. SPIE* **5181**, 62 (2003).
34. F. Xu, R. Tyan, P. C. Sun, C. Cheng, A. Scherer, and Y. Fainman, "Fabrication, modeling, and characterization of form-birefringent nanostructures," *Opt. Lett.* **20**, 2457 (1995).
35. R.-C. Tyan, A. A. Salvekar, H.-P. Chou, *et al.*, "Design, fabrication, and characterization of form-birefringent multilayer polarizing beam splitter," *J. Opt. Soc. Amer. A* **14**, 1627 (1997).
36. F. Xu, R.-C. Tyan, P.-C. Sun, Y. Fainman, C.-C. Cheng, and A. Scherer, "Form-birefringent computer-generated holograms," *Opt. Lett.* **21**, 1513 (1996).
37. W. Nakagawa, R.-C. Tyan, and Y. Fainman, "Analysis of enhanced second-harmonic generation in periodic nanostructures using modified rigorous coupled-wave analysis in the undepleted-pump approximation," *J. Opt. Soc. Amer. A* **19**, 1919 (2002).
38. W. Nakagawa, R. Tyan, and Y. Fainman, "Analysis of enhanced second-harmonic generation in periodic nanostructures using modified rigorous coupled-wave analysis in the undepleted-pump approximation," *J. Opt. Soc. Amer. A* **19**, 1919–1928 (2002).
39. U. Levy, C. H. Tsai, L. Pang, and Y. Fainman, "Engineering space-variant inhomogeneous media for polarization control," *Opt. Lett.* **29**, 1718–1720 (2004).
40. U. Levy, M. Nezhad, H.-C. Kim, C.-H. Tsai, L. Pang, and Y. Fainman, "Implementation of a graded-index medium by use of subwavelength structures with graded fill factor," *J. Opt. Soc. Amer. A* **22**, 724 (2005).
41. J. N. Mait, A. Scherer, O. Dial, D. W. Prather, and X. Gao, "Diffractive lens fabricated with binary features less than 60 nm," *Opt. Lett.* **25**, 381 (2000).

42. S. M. Rytov, "Electromagnetic properties of a finely stratified medium," *Sov. Phys. JETP* **2**, 466 (1956).
43. E. N. Glytsis and T. K. Gaylord, "High-spatial-frequency binary and multilevel stairstep gratings: Polarization-selective mirrors and broadband antireflection surfaces," *Appl. Opt.* **31**, 4459 (1992).
44. P. Lalanne and D. L. Lalanne, "Depth dependence of the effective properties of subwavelength gratings," *J. Opt. Soc. Amer. A* **14**, 450 (1997).
45. U. Levy and Y. Fainman, "Dispersion properties of inhomogeneous nanostructures," *J. Opt. Soc. Amer. A* **21**, 881 (2004).
46. C. C. Cheng, A. Scherer, R. C. Tyan, Y. Fainman, G. Witzgall, and E. Yablonovitch, "New fabrication techniques for high quality photonic crystals," *J. Vac. Sci. Technol. B* **15**, 2764 (1997).
47. H. C. Kim, K. Ikeda, and Y. Fainman, "Resonant waveguide device with vertical gratings," *Opt. Lett.* **32**, 539 (2007).
48. H. C. Kim, K. Ikeda, and Y. Fainman, "Tunable transmission resonant filter and modulator with vertical gratings," *J. Lightwave Technol.* **25**, 1147 (2007).
49. D. T. H. Tan, K. Ikeda, R. E. Saperstein, B. Slutsky, and Y. Fainman, "Chip-scale dispersion engineering using chirped vertical gratings," *Opt. Lett.* **33**, 3013 (2008).
50. V. R. Almeida, C. A. Barrios, R. R. Panepucci, and M. Lipson, "All-optical control of light on a silicon chip," *Nature* **431**, 1081 (2004).
51. K. Ikeda, M. Nezhad, and Y. Fainman, "Wavelength selective coupler with vertical gratings on silicon chip," *Appl. Phys. Lett.* **92**, 201111 (2008).
52. P. Yeh and H. F. Taylor, "Contradirectional frequency-selective couplers for guided-wave optics," *Appl. Opt.* **19**, 2848 (1980).